AD-A284 011

OFFICE OF NAVAL RESEARCH

CONTRACT N00014-92-C-0173

R&T Code 413309_ _ _01

Dr. Robert J. Nowak

Technical Report #11

Comparison of Water Models in Simple Electric Double Layers

by

Sheng-Bai Zhu, Michael R. Philpott, and James N. Glosli*

DTIC ELECTE SEP 0 6 1994 S D F

Prepared for publication in

Journal Chemical Physics

**IBM Research Division, Almaden Research Center,
650 Harry Road, San Jose, CA 95120-6099**

August 9, 1994

Reproduction in whole or in part is permitted
for any purpose of the United States Government

This document has been approved for public release
and sale; its distribution is unlimited

***Lawrence Livermore National Laboratory,
University of California, Livermore, CA 94550**

30pg 94-28891

94 9 02 313

SECURITY CLASSIFICATION OF THIS PAGE *(When Data Entered)*

REPORT DOCUMENTATION PAGE		READ INSTRUCTIONS BEFORE COMPLETING FORM
1. REPORT NUMBER 11	2. GOVT ACCESSION NO.	3. RECIPIENT'S CATALOG NUMBER
4. TITLE *(and Subtitle)* Comparison of Water Models in Simple Electric Double Layers		5. TYPE OF REPORT & PERIOD COVERED Technical Report
		6. PERFORMING ORG. REPORT NUMBER
7. AUTHOR(s) Sheng-Bai Zhu, Michael R. Philpott, and James N. Glosli		8. CONTRACT OR GRANT NUMBER(s) N00014-92-C-0173
9. PERFORMING ORGANIZATION NAME AND ADDRESS IBM Research Division, Almaden Research Center, 650 Harry Road San Jose, CA 95120-6099		10. PROGRAM ELEMENT, PROJECT, TASK AREA & WORK UNIT NUMBERS
11. CONTROLLING OFFICE NAME AND ADDRESS Office of Naval Research 800 North Quincy Street Arlington, VA 22217		12. REPORT DATE August 9, 1994 13. NUMBER OF PAGES 28
14. MONITORING AGENCY NAME & ADDRESS *(If different from Controlling Office)* Dr. Robert J. Nowak Office of Naval Research, Chemistry Division		15. SECURITY CLASS *(of this report)* unclassified 15a. DECLASSIFICATION/DOWNGRADING SCHEDULE

16. DISTRIBUTION STATEMENT *(of this Report)*
Approved for public release; distribution unlimited.

17. DISTRIBUTION STATEMENT *(of the abstract entered in Block 20, if different from Report)*

18. SUPPLEMENTARY NOTES

19. KEY WORDS *(Continue on reverse side if necessary and identify by block number)*

20. ABSTRACT *(Continue on reverse side if necessary and identify by block number)*
see next page

SECURITY CLASSIFICATION OF THIS PAGE *(When Data Entered)*

Comparison of Water Models in Simple Electric Double Layers

Sheng-Bai Zhu and Michael R. Philpott
IBM Research Division
Almaden Research Center
650 Harry Road
San Jose, CA 95120-6099

James N. Glosli
Lawrence Livermore National Laboratory
Livermore, CA 94550

August 9, 1994

Accesion For
NTIS CRA&I
DTIC TAB
Unannounced
Justification
By
Distribution /
Availability Codes
Dist | Avail and / or Special
A-1

Abstract

The three bulk water models (SPCE, TIP4P and ST2) are compared in molecular dynamics simulations of electric double layers consisting of a monovalent ion (Na^+ or Cl^-), water as solvent, and a flat metal electrode. The goal is to identify features of the double layer that are sensitive to the model and those that are not. The simulations are done with zero external field and one non-zero applied field. All electrostatic image interactions due to the ion and the point charges constituting the water molecules are included in the calculation. All the models give rise to several well defined solvent density oscillations at the metal surface and the first peak in particular can be strongly accentuated by an external electric field. The Na^+ ion occupies a diffuse zone in which its first solvation shell remains intact even when drawn to the electrode by an external field. One striking difference occurs for the ST2 water compared to the other models. In a cathodic external field the Na^+ ion does not concentrate near the electrode. There are

also quantitative differences in the electric potential profiles. Effects of replacing N ith Cl^- are also studied. It was observed that there was less struc n the water density profiles with solvated anions. The Cl^- ion occupies a diffuse zone that extends to the surface where it makes occasional contact and its solvation shell greatly distorted. In an external field the chloride ion forms a compact layer at the metal with no diffuse component to its distribution. Significant differences in using different water models are observed and are interpreted on the basis of the relative strength of the solvation and the stiffness of the liquid.

1 Introduction

In this paper we use constant (N, v, t) molecular dynamics computer simulations to study the sensitivity [1, 2] of the main properties of electric double layers to the model used. The same model for the metal electrode is used throughout. The ion parameters were those optimized for the bulk solutions. We will show that all the models have major solvent structural features in common, with the simple point charge (SPCE) model and the transferable intermolecular potential (TIP4P) model being similar in many respects. The importance of this work is in identifying model independent features likely to exist in real systems and differences associated with particular models. All electrostatic interactions between ions and water and the electrostatic images of ions and water in the model are included in the calculation.

Electric double layers are formed when aqueous ionic solutions contact charged plates. The ions migrate toward the charged surface until the field of the surface charge is completely shielded outside a narrow zone (less than a few nanometers thick at 0.1 M salt concentration) next to the metal. The region where zero average field begins marks the edge of the bulk electrolyte. In the bulk region the electrolyte solution is neutral, the average electric field is zero, and the water molecules are not preferentially oriented. According to the traditional electrochemical textbook model [3, 4, 5], the electric double layer consists of a diffuse part of mobile ions and water stretching into the bulk electrolyte and a compact part comprising the charged metal surface region and contact adsorbed species. In the diffuse layer, fully hydrated ions move under the combined influence of thermal forces from neighboring species and interactions with metal plates as well as external fields. Distri-

butions in the diffuse layer are described by the Gouy-Chapman theory [6, 7] which takes no account of the detailed nature of the ions other than the magnitudes of their charges and treats the solvent as a continuous fluid with given dielectric constant. In the compact layer, if one exists for the system under study, ions physisorb without electronic discharge or chemisorb and form a bond with some degree of covalent character [4]. In this part of the electric double layer, the properties have been described by the Stern [8], Frumkin [9], Grahame [10], or Bockris, Devanathan, and Muller [11] models. In particular the Bockris, Devanathan, and Muller model [11] assumed the compact region consisted of two layers of solvent containing contact adsorbed ions. An obvious disadvantage of the traditional model is the absence of predictions concerning water (the majority species!) perturbations due to visiting counter ions, the loss of some or all of the solvation sheath of contacting ions, and the formation of chemical bonds between ions, water and the surface.

During the last fifty years the traditional model evolved through the analysis of numerous experiments designed to measure surface coverages as a function of electrolyte composition and externally applied potential. Recent UHV experiments [4] have revealed that some of the traditional views regarding contact adsorption must be reassessed, for example, iodide ions discharge on Pt(111) surfaces at high coverage. Problems concerning change in electronic structure with coverage are beyond the scope of the present paper. However classical molecular dynamics computer simulations can add detailed insights at the atomic scale, including information about the temporal and structural aspects of molecular organization in the electric double layer. In these systems water molecules are perturbed by ions, external fields, and the atoms making up the solid surface. There is a growing literature describing computer simulations of water in perturbed systems. Subjects of recent studies are: aqueous electrolyte solutions, pure water near charged or uncharged surfaces, and water-ion complexes in the vicinity of charged or uncharged surfaces. A recent review of water in perturbed states has been published by Zhu and coworkers [12].

All the computer simulations of double layer problems so far published have used water models developed for the bulk state. Most of these models are within the framework of pairwise additive potentials which treat the polarization effect in an average way through effective charges. An important question naturally arises: whether the mean field approximation is still a valid

description, or to what extent it is a reasonable description, for studying perturbed water where the molecular environment is spatially inhomogeneous. There is, unfortunately, no straightforward answer for this question since microscopic information of double layers has not been available from current experiments and the existing water models can only reproduce at most a few experimental data. They may be appropriate in some aspects but inappropriate in others. The lack of a criterion for the 'truth' causes difficulty in directly testing the reliability of a water model for solving electric double layer problems. In this paper, we simply compare molecular dynamics simulation results of three most commonly employed water models, namely SPCE [13], TIP4P [14], and ST2 [15], in otherwise identical conditions. These models respectively represent a three-site, four-site, and five-site version of rigid and non-polarizable water molecules. Particular attention will be paid on differences and similarities of the simulation results. If the results are qualitatively different, at least one of these models is inappropriate in describing the properties studied. On the other hand, similarities in results indicate these models are almost equivalent in these aspects. It, of course, does not necessarily mean that these properties really correspond to real physical features of electrolytes near charged solid surfaces.

2 Model

In each simulation the cell contained a single ion, either Na^+ as the cation or Cl^- as the anion (0.35 M concentration), and a total of 157 water molecules, sandwiched between two walls one representing the metal electrode and the other the neutral restraining wall. The cells are replicated to infinite parallel to the xy plane of the metal. We call this the immersed electrode model [16]. In this model, a full treatment of all electrostatic interactions is performed. This means interactions between the ion, all the water molecules, and all the electrostatic images of the ion and all the water molecules (due to the presence of a single metal surface). In the absence of an external field the net charge on the metal electrode is the image charge of the ion in the aqueous subphase, which has a fluctuating position and is opposite in sign to that of the ion. The total charge on the metal in the case of Na^+ was $q_T = q_{im} = -e$, where e denotes the electron charge. A very high surface electric field exists across the metal-solution interface, which drops rapidly to zero as the

dielectric boundary is approached. The water molecules were represented by one of the three models mentioned above, and the ion parameters were chosen to be consistent with the water model. All these water models have been used extensively to study liquid water and electrolyte solutions and all have reasonable success in explaining selected bulk phase properties. To stress the system and mimic the effect of even higher salt concentration on the water layers near the electrode we also performed calculations with an external electric field applied in a direction that reinforced the existing field due to the ion and its electrostatic image. The total charge on the metal in the case of Na^+ was $q_T = q_{im} + q_{ext} = -2e$ with the uniformly distributed component $q_{ext} = -e$. Although systems under external electric field do not exist at equilibrium in nature, we consider this a useful ploy to examine how system responds initially to a change in field, and as shown by Philpott and Glosli [16], how even higher same ion concentrations alter the water structure next to the electrode.

Several approximations are implicit in the present study. Through the use of bulk water models, a basic assumption involved in the non-polarizable water models is that the molecular environment is spatially isotropic so that the polarization effects may be treated in an average way by introducing effective point charges. This assumption will break down when 'perturbations' from neighboring solutes, external fields, interfaces etc., deviate greatly from the mean field of the bulk phase. It seems reasonable to think this will occur when the molecule is in the first layer next to the electrode. Also omitted here are the geometric distortions of the molecular framework which may be significant in the presence of intense fields [17, 18, 19, 20, 21] such as the cases occur around polyvalent ions. We can only minimize this effect here by restricting the systems studied to monovalent ions. The rigid geometry and the absence of polarizability mean that the dipole moment is fixed at a mean value appropriate for the bulk phase. In turn this means that dielectric saturation could occur in smaller electric fields than observed experimentally, and will be manifest by completely oriented water molecules. For each system, the ion-water interactions were optimized on the basis of bulk phase. It is therefore to be expected that the results obtained from different model calculations may be differentiated when interfacial phenomena are investigated. Our general goal is to examine the consistency of these models in describing the properties of electric double layers.

The water-ion mixture is confined between flat featureless plates 1.862

nm apart. The left hand plate (see Fig. 1) at z = -0.931 nm is a dielectric, it interacts with all molecules and ions by the 9-3 potential of Lee, McCammon, and Rossky [22]. This potential represents the interaction of water and ions with the core electrons of the wall. The explicit form of the water-wall and ion-wall 9-3 potentials for a solid with density ρ is [23]:

$$u_{9-3} = 2\pi\rho\epsilon_w\sigma_w^3\left[\frac{2}{45}\left(\frac{\sigma_w}{z-z_w}\right)^9 - \left(\frac{\sigma_w}{z-z_w}\right)^3\right], \tag{1}$$

where ϵ_w and σ_w are the Lennard-Jones energy and radius for the wall potential. The coordinate z, measured perpendicular to the interface, is the distance of the mass center of ion or the distance of the oxygen atom of the water molecule. This choice of wall potential neglects the interaction of the hydrogen atoms with the wall. The right hand plate at z = 0.931 nm represents a metal surface. In addition to the same 9-3 potential for core interactions, the interaction of charges on ions or on the charge sites inside each water molecules with conduction electrons is modeled by an electrostatic image potential. For all these systems, the image plane is chosen to be coincident with the origin plane of the 9-3 potential, which passes through the nuclei of the metal atoms on the first layer at z = 0.931 nm.

A number of schemes have been developed in past years to treat long range electrostatic fields. In this work, we employ the fast multipole method (FMM) proposed by Greengard and Rokhlin [24, 25, 26, 27], which is computationally more economical than the Ewald summation [28, 29, 30] and, compared with other methods, is easy to use in combination with complex boundary conditions [31, 32]. Additionally it is well suited to vector and parallel machines, and the error in computation is controlled by changing the number of terms retained in the multipole expansions. The first application of FMM to electrochemical problems were the molecular dynamics calculations of dielectric constant of bulk SPCE water by Glosli and Philpott [32].

Table 1 lists the potential parameters employed for the systems studied in this paper, together with the relevant references. Here ϵ_O and σ_O represent the Lennard-Jones energy and radius of water-water interaction, ϵ_{OI} and σ_{OI} label the same quantities for the ion-water interaction. For systems in an external electric field, the additional electric field strength in vacuum was 5.22×10^7 V/cm, equivalent to a surface charge density of 0.288 e/nm^2.

Although, on average, the electrostatic image of the ion has the same surface charge density, its influence on the solution depends on the behavior of the ion and, therefore, is not exactly identical with the external field.

Constant (N, V, T) molecular dynamics calculations were performed on each system, for simulation times of one nanosecond in all cases except the system Na^+ in ST2 water where the calculation was run for 2 ns. This provided a cross-check to against artifacts from poor statistics. A time step of 2 fs is used for integrating the equations of motion. For each simulation, the first 100 ps was used to equilibrate the system at a temperature of 294K, and the remainder is to accumulate data. The sample box is a cube with the edge length of 1.862 nm and was periodically replicated along the x and y directions parallel to the electrode surface.

3 Results and Discussion

In this section the results of the simulations are presented in terms of probability distributions for the chemical components (water, H atoms and ions) averaged over the x and y directions. After averaging the distributions, which we will also refer to loosely as density profiles, show only a dependence on z, the coordinate perpendicular to the surface. They usefully characterize the main structural features of the electric double layers. In addition, we have calculated the total microscopic charge and the z component of the dipole moment of water (vector component parallel to the surface normal). For convenience we first discuss systems containing Na^+ and Cl^- separately and later focus on points of difference. Some large differences are to be expected because asymmetry in the water models and the reversal in the interfacial field for cations compared with anions.

3.1 Systems Containing Na^+ Ions

Figures 1 to 3 display the basic results. The solid curves correspond to no external field, a physically acceptable state. The combination of broken and solid lines indicate the main change occurring when a field is turned on. This external static electric field is always in the direction to pull the ion to the metal surface, so that the total surface field could be as high as 10 GV/m. As has been shown elsewhere [16], the field at the metal surface

(only) is equivalent to having an extra ion in the system. For additional emphasis in all the figures presented in this paper, the label 'e' signifies how the distributions change in the presence of the external field. Broken vertical lines at $|z| = 0.682$ nm, indicate the location of the 'effective' walls which are defined as the planes parallel to the solid surfaces where the 9-3 wall potential crosses zero. In each figure, the metal electrode is on the right side with the image plane on the extreme edge of the figure ($z = 0.931$ nm), and the uncharged restraining (dielectric) wall is on the left at z = -0.931 nm.

We discuss the main features first starting with the majority species water. In surveying the results plotted in Figures 1 to 3 we conclude that the water and proton distributions calculated for all three models are in basic qualitative agreement. In zero external field, the water distributions are slightly asymmetric with respect to the central plane ($z = 0$). This difference is due to the charge-image charge interaction, and arises from the intrinsically different nature of the solution-surface interactions occurring at the metal surface compared to the dielectric surface. The effect on the density profiles is weak for neutral water and strong for the H atoms.

All three water density profiles exhibit broad maxima at -0.5, -0.2 (indistinct), 0.3 and 0.6 nm. These peaks, due to layering at the surfaces are more distinct on the metal side ($z > 0$). In all three figures there is a small sharp peak on the edge of the profile near 0.7 nm. It is most visible in Figures 2 and 3 for TIP4P and ST2 models. When the field is turned on it becomes the sharpest feature in the water profile. This peak is due to a few water molecules with mass centers localized near 0.68 nm at the edge of the repulsion zone. We address the question of how the orientation of these water molecules differs from the majority of waters near the surface after describing the proton (H atom) distributions.

As with water center of mass, the H atom distributions are very similar for all three models. There is asymmetry with respect to $z = 0$. This is especially true on the metal side because our model allows H atoms to get closer to the image plane. The main peaks are at 0.2 (broad), 0.55 (broad) and 0.76 nm (sharp). The proton peak at ca. 0.76 nm is particularly distinct because these protons are attracted by a strong image electrostatic field and since they do not feel the 9-3 wall potential directly, they can penetrate the exclusion zone for the oxygen and ions created by the repulsive 9-potential. The peak at 0.76 nm is clearly associated with water molecules of mass center near 0.68 nm. When the field is turned on, the electric field near the metal surface

is almost doubled and so more protons are attracted to the metal and the 0.76 nm peak doubles in height. The height of the first peak in the hydrogen number density ρ_H is about 90% of that in the oxygen number density ρ_O and their peak-to-peak separation is about 0.08 nm. In addition, the ratio of the number of hydrogen atoms in the first layer (defined as the portion between the first peak near the metal surface and the corresponding liquid-solid interface) to the number of oxygen atoms in the first layer (similarly defined) is about 0.6. These values suggest there is a large probability to have one proton pointing at the metal rather than having the dipole aligned perpendicular to the surface (the ultimate high field configuration).

It is natural to ask if the packing of water molecules next to the metal is increased. In the absence of strong surface electric fields, the interfacial water molecules tend to be oriented with some of their hydrogen atoms pointing away from the liquid phase, and some involved in H-bonding to a second layer [22]. The orientational ordering and packing of the water molecules near the metal surface is disrupted by the high surface electric field between the ions and their images, with the result that some hydrogen bonds break allowing more water molecules to pack closer. The increased local density of water is the expected packing phenomenon in the interfacial region, resulting from the hydrogen bond breaking. Also some solvent structure breaking will occur because of disruption due to the proximity of the cation.

Next we discuss the z component of dipole density profile. The three models show similar behavior near the metal with and without an applied external field. For all the models there is a prominent peak at 0.68 nm from oriented water at the surface. As expected the peak has a tail towards the bulk side signifying a decrease in orientation as the distance from the surface increases. In the interior of the film the dipole density drops to a low value signifying shielding of the charge of ions and their images. In the applied field the dipole profile is peaked at both surfaces (edge effect) and for $|z| < 0.6$ nm is approximately uniformly polarized. This latter behavior is as expected for a dielectric exhibiting orientational polarization. In zero field the peak at 0.68 nm arises because of orientational saturation at the position where the electric field due to the ions is greatest. There is also a weak broad maximum between 0.2 and 0.4 nm due to ion induced orientation of the water molecule. The model ST2 shows a distinctive difference near the second boundary z = -0.931 nm. There is practically no dipole oscillation at -0.68 nm. Models SPCE and TIP4P have a small but significant variation in dipole density

between -0.7 and -0.6 nm compared to ST2. As a result for the different models, the electric potential will vary in significantly different ways in the range $-0.931 < z < -0.4$ nm.

We have also calculated the total charge density across the system. Though we do not show it in the figures we describe it briefly. Most noticeable are oscillations presumed due to water packing variations. For the Na^+-water systems without external electric field, the two planar models, SPCE and TIP4P, produce almost identical total charge density ρ_q. In both models ρ_q display a prominent peak near the electrode, followed with a deep minimum. Some small difference in ρ_q may come from the shift of the negative charge in TIP4P. The main structure in the charge density ρ_q near the wall comes from oriented and localized water molecules. There is a peak (at 0.76 nm) in ρ_q contributed from the hydrogens, coincidence with the first peak in ρ_H at approximately 0.76 nm. Since the density profiles for the hydrogen atoms and water molecules are relatively insensitive to the water model, the difference in the peak amplitude of ρ_q must be mainly a consequence of the different charge value carried by the hydrogens. Indeed, the partial charge carried by the hydrogen nuclei in ST2 is almost one half of those in SPCE and TIP4P, and the peak in ρ_q is reduced by about the same ratio. Another effect that perturbs the charge density profile is the molecular geometry. For the ST2 molecule, the negative charges are moved along the tetrahedral directions by 0.08 nm. This causes a shallower minimum near the metal wall, shifted towards the center of the film. Such contributions also affect ρ_q near the dielectric wall. However, the minima in systems Na^+/ST2 and Na^+/ST2/e (field on) differ with the other four to an even larger extent partly because of the contribution made by the sodium cation.

The largest differences among these systems are the ion density profiles, which play an important role in determining the electric field and potential across the system. In the absence of the applied field, the ions are completely hydrated all of the time and range across the greater part of the film. The sodium ion in ST2 water is localized from $\sim$ -0.3 to 0.3 nm. It shows some propensity to contact the metal surface in the SPCE or TIP4P water molecule systems.

However, the situation becomes qualitatively different in an external field. Although some small shift towards the metal surface is observed for SPCE, the cationic density profiles calculated for systems Na^+/SPCE and Na^+/TIP4P are almost superimposable. In the systems SPCE and TIP4P

there is a reasonable probability for Na^+ to make solvent-bridged contact to the metal surface, a central feature of the Grahame model [10] of the electric double layer. For TIP4P solvent, the probability is slightly reduced. However, for ST2 water there is a greatly reduced probability for the primary solvent shell contacting the electrode. The density profile of the sodium ion looks flat, contrasting the changes observed in the other systems where the surface electric field draws the ion towards the metal. There is some small probability that the cation weakly adsorbs on the dielectric surface, along with its primary solvation sheath (splayed). No contact adsorption is observed on the metal surface.

The entirely different behavior for ions observed in the planar solvents SPCE and TIP4P compared to the three dimensional ST2 solvent molecule is very important since it influences the conclusion about the nature of the adsorbed ions. In order to avoid possible artifacts introduced from poor statistics and/or equilibrium, we doubled the simulation time for the system Na^+/ST2 from 1 ns to 2 ns and observed no significant changes. This confirms that the simulation results should be qualitatively reliable and previously described effect real for this model.

3.2 Systems Containing Cl^- Ions

In figures 4 to 6 the probability profiles for the three water systems and chloride are shown. In the absence of an external field we observe no qualitative differences among the three models. A contributing factor is the larger radius of the chloride ion and weaker primary hydration.

The main peaks of ρ_{H_2O} are broad and are located at -0.6, 0.3 and 0.6 nm. There is a hint of a broad peak between -0.2 and -0.3 nm in ST2 water. Along the series SPCE, TIP4P to ST2 a small peak grows in near 0.65 nm on top of the broader peak at 0.60 nm. In the presence of the applied field, the left shoulders of ρ_{H2O} are raised in the same order. This structure resembles the one seen in the cation systems in shape and position. Careful inspection shows that for anions this weak peak is always at smaller z. The shift is due to the reversal in the orientation of water in the surface electric field generated by the anions.

In the external field, the 0.65 nm peak grows in sharply, becoming the sharpest feature in the water profile. However the peak is not as sharp or intense as in the case of sodium ions discussed in the last section. The reason

is because the chloride ion contact adsorbs in the applied field there is a drop in the electric field on the left side of the ions so that the field experienced by the water molecules in the first layer is weaker by approximately a factor two (this is in contrast to the sodium ion case where the field due to the ions decays slowly over the diffuse region).

In zero field, the H atom profiles are similar. The main peaks occur at -0.6 (edge), 0.3, and 0.6 nm (main peak). The ST2 model has an additional broad maximum near -0.2 nm. The main peak at 0.6 nm also grows by approximately a factor two (compared to ρ_{H_2O}). In the applied field both protons are repelled and their is no evidence that the distributions split as in the case with cation fields. A new feature in the H distributions in the external field is the appearance of a small distinct peak at -0.75 nm. In the applied field the water molecules orient across the film so that protons poke outward at the dielectric boundary.

Unlike the situation for the Na^+-water systems, the density profiles of ion for the Cl^--water systems shown in Figs. 4-6 are all quite broad and diffuse and show little variation with model. The difference between the adsorption behavior of anion and cation becomes larger in the external electric field because all the chlorides localize on the electrode. In zero field, the Cl^- density profiles are all diffuse with a small but finite chance for contact adsorption. When the anodic external electric field is applied, all the anions strongly contact adsorbed on the metal surface. In the SPCE or TIP4P environment, the anion is very seldom found far from the electrode, though there is a small statistical probability that the anion will desorb temporarily in the case of TIP4P. When the adsorbed chloride peak heights are compared, it is seen that chloride density profile ρ_{Cl} in ST2 (see Figure 6) has the highest amplitude and narrowest full width at half maximum, implying most localization in this case.

The dipole density for water, ρ_D, shown in Figures 4-6 indicate that the orientational ordering of the water molecules from the three models do not deviate from each other significantly except at the dielectric surface. As discussed earlier in the case of the sodium ion, the ST2 dipole profile is much flatter coming off the dielectric wall. The similarity in the rest of the zero field profile stems from similarities in the chloride ion distributions. When the external field is applied, the dipole distribution functions are similar to the situation in pure water because in each model the ion is localized (contact adsorbed) entirely on the metal. The peaks near $|z| = 0.65$ nm are from 'end

effect' due to the walls and on the metal side they are also caused by intense surface field contributed from the chloride ion.

3.3 Further Discussions

It is well known [36] that the adsorption behavior is, to a large extent, controlled by the competition among the ion-water, ion-surface, water-water, and water-surface interactions. Referring to Table I where the potential parameters used in the simulations are given, we find that the differences in ϵ_{OI} and σ_{OI} between systems Na^+/SPCE and Na^+/ST2 are much smaller than those between systems Na^+/SPCE and Na^+/TIP4P. Therefore, the differences in behavior of Na^+ ions seen in ρ_{Na} cannot be due to the spherically symmetric Lennard-Jones potential. It must therefore be a consequence of some angular-dependent interactions. At small distances the Coulomb interaction between ion and water depends strongly on the model employed because of their different geometries and charge distributions, and consequently different higher multipole moments.

For a better understanding of the electrical properties, we plot the electrical potential profiles across the electrolyte in Fig. 7, setting the average of the potential on the dielectric plate to be zero, as a reference point. The electrical potential profiles are calculated from the charge distribution along the z direction. These curves show that the electrical potential in the central part ($|z| \lesssim 0.6$ nm) of the Na^+/ST2 and Cl^-/ST2 films without external field are nearly zero, while for systems Na^+/SPCE, Na^+/TIP4P, Cl^-/SPCE, and Cl^-/TIP4P, the potential drops by almost -0.6 V. In this sense, the central parts of systems Na^+/ST2 and Cl^-/ST2 display approximately bulk behavior. There is no such region in the SPCE and TIP4P solutions. A simple interpretation of the phenomenon is based on the well-known fact that the bulk ST2 water is more structured than SPCE and TIP4P. Therefore, the former persists under the perturbation, while the latter two are more fragile.

In accord with the polarization and net charge distributions described earlier, the electric potentials for systems Na^+/SPCE and Na^+/TIP4P in zero field have two minima around $|z| \approx 0.6$ - 0.65 nm. In the presence of the applied field, the minima around the metal surface are about 600 mV deep, while for system Na^+/ST2, it is much shallower. This explains the broad unstructured diffuse region occupied by the cation and its hydration shell in

system Na^+/ST2/e described above.

In all the cases studied, the hydration shell of Na^+ was complete. We have calculated pair correlation functions for the ions and water molecules. It is interesting to note that the first peak of Na^+-TIP4P pair correlation function is located near 0.25 nm, much larger than the mixed Lennard-Jones radius of 0.19 nm (see Table I). This would imply that the solvation structure of Na^+-TIP4P is relatively weak. In contrast, the first peak of the Na^+-ST2 radial distribution function is located at $\sim$ 0.24 nm, much shorter than the mixed $\sigma_{OI} = 0.273$ nm, indicating a strong attractive electrostatic interaction on average. The hydration numbers for systems Na^+/ST2 in zero and non-zero external field are almost 20% higher than those of the other four systems.

In contrast to the cation solutions, the hydration number for Cl^- decreases in the order of SPCE, TIP4P, and ST2. The propensity of Cl^- to adsorb on the surface increases in the same order, as expected. Because of the anionic adsorption, there is a significant reduction in the hydration number when the external electric field is turned on. Since the interaction of Cl^- with the ST2 molecule is weaker than the interactions with the other types of solvent molecules, there is a greater loss in the first hydration shell for ST2 ($\sim$ 32%) than for SPCE ($\sim$ 26%) and TIP4P ($\sim$ 24%).

According to the calculation of bulk solution by Heinzinger [35], the ST2 water molecules in the first hydration shell of Na^+ ion are oriented with strong preference to form a tetrahedral structure. For planar water molecules such as SPCE and TIP4P, the hydrated ion has the largest probability to be located in the same plane of the water molecule. As pointed out by Heinzinger [35], the preferential orientation of water molecules in the first hydration shell of an ion belongs to one of the rare cases where the simulation results depend sensitively on the model employed. All these results consistently show that the potential models with stronger angular dependence like ST2 form stiffer hydration shells compared to less structured liquids such as SPCE and TIP4P. Our simulation results also show that the hydration structure of cations in ST2 solution does not vary with the external field, whereas in SPCE and TIP4P solutions there were some changes albeit small ones. The discussion thus far suggests that the cation-water interaction, especially in the case of ST2 solution, is very strong compared to the interactions with the metal wall. Therefore, the movement of the hydrated cation is accompanied with the surrounding water molecules. On average, more water molecules in the ST2 medium than in the SPCE or TIP4P media move with the cation.

The interaction between Na^+ ion and ST2 water is stronger than in the case of SPCE or TIP4P water and the ST2 liquid is more strongly hydrogen-bonded. As a consequence, there is a greater tendency for Na^+ to be hydrated in the ST2 environment than adsorb to the electrode.

4 Conclusions

Molecular dynamics simulations were performed on two different ions in three different water models, with zero applied field and with an external applied field. All electrostatic interactions between ions, water molecules, and their electrostatic images in the metal have been accurately computed with the FMM. Our goal was, through detailed comparison of the computed results, to gain some insight concerning the relative usefulness of these models at aqueous interfaces. These models have been initially developed in the bulk phase and later have been widely applied to studying water in perturbed states. The application to surface problems may invalidate some implicit approximations involved in their original derivations (in particular, the use of fixed charges). For the most part it was found that the density profiles of the water properties are relatively insensitive to the models, though there were some discrepancies that were discussed in the last section. Since the charges are buried inside Lennard-Jones spheres their influence on the dynamics is muted. This is not so in the case of electrical properties. Even cursory examination of Figures 1 to 6 shows that the dipole density profiles vary much more from model to model than do the water and hydrogen density profiles. This is due, in part, to the different molecular geometry and charge distribution in these models, and in part to energetic competition among various interactions.

Some common features in the water structure were observed for the three models. In particular, the water structure near the metal surface was sensitive to the magnitude and direction of the surface field. In the absence of an external field the surface electric field arises primarily from the density profile of the ion. If the ion is not contact adsorbed then the surface water molecules see a large field that disrupts H-bonds and orients water dipoles with the field. Contact adsorbed ions are less effective because their high field region lies closer to the surface and contains few molecules. The variation in water density peaks with external field verifies this conclusion.

In the absence of the electric field, the ionic solute, whether positively or negatively charged, distributes diffusely. Greater variation is found for the hydrogen density profiles, suggesting the occurrence of molecular reorientation under the influence of the electric field of the ions. Applying the external field further increases the molecular alignment. Because of the strong Coulomb interaction between the charges and their images, the interfacial water molecules are bound to the metal surface, giving rise to a higher density layer. This was also seen in earlier simulations of similar systems [16, 37, 38, 39, 40, 41].

An interesting conclusion of the present work is the qualitatively different adsorption behavior of the sodium ion in different media. In ST2 solution the cation is strongly hydrated and does not adsorb as testified by the density profile. In contrast, in the SPCE and TIP4P environments, it shows a strong propensity to be adsorbed via the first hydration shell. The adsorption behavior of the anion is strongest for ST2 and weakest for the other two. This variation is related to the hydration structure which reflects the energetic competition between water-ion and water-water interactions. This raises an important question whether a model based on effective potentials in the bulk state is a reasonable approximation in studying the electric double layer problems? Some properties are insensitive to the model and can be well described by simple models, but others are not. Of course, studying two ions does not provide enough information to decide. What is need are calculations for a series of related cations and anions. Such calculations have been performed for alkali metal and halide ions in ST2 water [42] where we have learned that many known electrochemical trends can be modeled. However what we learn from this work is that details in these trends are going to be very model sensitive until new models are developed for water and ions that address the peculiar aspects of interfaces. In particular we need a model that incorporates electric polarizability and attributes that mimic weak chemisorption [43].

References

[1] S.-B. Zhu and C. F. Wong, J. Chem. Phys. 98, 8892 (1993).

[2] S.-B. Zhu and C. F. Wong, J. Chem. Phys. 98, 9047 (1993).

[3] J. O'M. Bockris and S. U. Khan, *"Quantum Electrochemistry"* (Plenum Press: New York, 1979).

[4] A. T. Hubbard, Chem. Rev. 88, 633 (1988).

[5] R. Parsons, Chem. Rev. 90, 813 (1990).

[6] G. Gouy, J. Phys. 9, 457 (1910).

[7] D. L. Chapman, Philos. Mag. 25, 508 (1913).

[8] O. Stern, Z. Electrchem. 30, 508 (1924).

[9] A. N. Frumkin, Trans. Faraday Soc. 36, 117 (1940).

[10] D. C. Grahame, Chem. Rev. 41, 441 (1947).

[11] J. O'M Bockris, M. A. V. Devanathan and K. Mueller, Proc. Roy. Soc. (London) A274, 55 (1963).

[12] S.-B. Zhu, S. Singh, and G. W. Robinson, Adv. Chem. Phys. 85(3), 627 (1994).

[13] H. J. C. Berendsen, J. R. Grigera, and T. P. Straatsma, J. Phys. Chem. 91, 6269 (1987).

[14] H. J. Jorgensen, J. Chandrasekhar, J. D. Madura, R. W. Impey, and M. L. Klein, J. Chem. Phys. 79, 926 (1983).

[15] F. H. Stillinger and A. Rahman, J. Chem. Phys. 60, 1545 (1974).

[16] M. R. Philpott and J. N. Glosli, in *"Theoretical and Computational Approaches to Interface Phenomena"*, Eds. H. Sellers and J.T. Golab (Plenum Press: New York, 1994).

[17] P. Bopp, Pure & Appl. Chem. 59, 1071 (1987).

[18] S.-B. Zhu and G. W. Robinson, Z. Naturforsch. 46a, 221 (1990).

[19] S.-B. Zhu and G. W. Robinson, J. Chem. Phys. 94, 1403 (1991).

[20] S.-B. Zhu, J.-B. Zhu, and G. W. Robinson, Phys. Rev. A44, 2602 (1991).

[21] S.-B. Zhu and G. W. Robinson, J. Chem. Phys. 97, 4336 (1992).

[22] C. Y. Lee, J. A. McCammon, and P. J. Rossky, J. Chem. Phys. 80, 4448 (1984).

[23] W. A. Steele, Surf. Sci. 36, 317 (1973).

[24] L. F. Greengard, *"The Rapid Evaluation of Potential Fields"* (MIT Press: Cambridge, MA, 1987).

[25] L. Greengard and V. Rokhlin, J. Comp. Phys. 73, 325 (1987).

[26] J. Carrier, L. Greengard, and V. Rokhlin, Siam J. Sci. Stat. Comput. 9, 669 (1988).

[27] L. Greengard and V. Rokhlin, Chemica Scripta A29, 139 (1989).

[28] P. P. Ewald, Ann. Physik 54, 519 (1917).

[29] P. P. Ewald, Ann. Physik 54, 557 (1917).

[30] M. Born and K. Huang, *"Dynamical Theory of Crystal Lattices"* (The Clarendon Press: Oxford, England, 1954).

[31] J. N. Glosli, Unpublished results.

[32] J. N. Glosli and M. R. Philpott, Proceedings of the Symposium on *"Microscopic Models of Electrolyte Interfaces"*, Vol. 93-5, 80 (The Electrochemical Society, Inc.: Pennington, 1993).

[33] J. Caldwell, L. X. Dang, and P. A. Kollman, J. Am. Chem. Soc. 112, 9144 (1990).

[34] J. Chandrasekhar, D. C. Spellmeyer, and W. L. Jorgensen, J. Am. Chem. Soc. 106, 903 (1984).

[35] K. Heinzinger, Physica, B131, 196 (1985).

[36] J. O'M. Bockris and A. K. N. Reddy, *"Modern Electrochemistry"* Vol. 2 (Plenum Press: New York, 1973).

[37] J. N. Glosli and M. R. Philpott, J. Chem. Phys. 96, 6962 (1992).

[38] J. N. Glosli and M. R. Philpott, Proceedings of the Symposium on *"Microscopic Models of Electrolyte Interfaces"*, Vol. 93-5, 90 (The Electrochemical Society, Inc.: Pennington, 1993).

[39] J. N. Glosli and M. R. Philpott, J. Chem. Phys. 96, 6962 (1993).

[40] D. A. Rose and I. Benjamin, J. Chem. Phys. 95, 6856 (1991).

[41] T. Matsui and W. L. Jorgensen, J. Am. Chem. Soc. 114, 3220 (1992).

[42] M. R. Philpott and J. N. Glosli, unpublished calculations

[43] S.-B. Zhu and M. R. Philpott, J. Chem. Phys. 100, 6961 (1994) Interaction of Water with Metal Surfaces, submitted December 93.

Table 1 Potential Parameters

Water	Ion	ϵ_O (kJ/mol)	σ_O (nm)	ϵ_{OI} (kJ/mol)	σ_{OI}	Ref.
SPCE	Na^+	0.650	0.316	0.544	0.216	[33]
SPCE	Cl^-	0.650	0.316	0.418	0.432	[33]
TIP4P	Na^+	0.649	0.315	6.724	0.190	[34]
TIP4P	Cl^-	0.649	0.315	0.493	0.442	[34]
ST2	Na^+	0.317	0.310	0.358	0.273	[35]
ST2	Cl^-	0.317	0.310	0.168	0.486	[35]

Figure Captions

Fig. 1 Density profiles of water molecules, their hydrogen atoms, the ion, and the orientational polarization of the water molecules for System Na^+-SPCE. The label e indicates the results obtained in the presence of the applied field.

Fig. 2 Density profiles of water molecules, their hydrogen atoms, the ion, and the orientational polarization of the water molecules for System Na^+-TIP4P. The label e indicates the results obtained in the presence of the applied field.

Fig. 3 Density profiles of water molecules, their hydrogen atoms, the ion, and the orientational polarization of the water molecules for System Na^+-ST2. The label e indicates the results obtained in the presence of the applied field.

Fig. 4 Density profiles of water molecules, their hydrogen atoms, the ion, and the orientational polarization of the water molecules for System Cl^--SPCE. The label e indicates the results obtained in the presence of the applied field.

Fig. 5 Density profiles of water molecules, their hydrogen atoms, the ion, and the orientational polarization of the water molecules for System Cl^--TIP4P. The label e indicates the results obtained in the presence of the applied field.

Fig. 6 Density profiles of water molecules, their hydrogen atoms, the ion, and the orientational polarization of the water molecules for System Cl^--ST2. The label e indicates the results obtained in the presence of the applied field.

Fig. 7 Electric potential profiles calculated from the charge distributions. The curves for systems Na^+/SPCE and Na^+/SPCE/e are very similar to the curves for systems Na^+/TIP4P and Na^+/TIP4P/e and so are not shown in this figure. The electric potential profiles for systems containing Cl^- ion has a similar behavior.

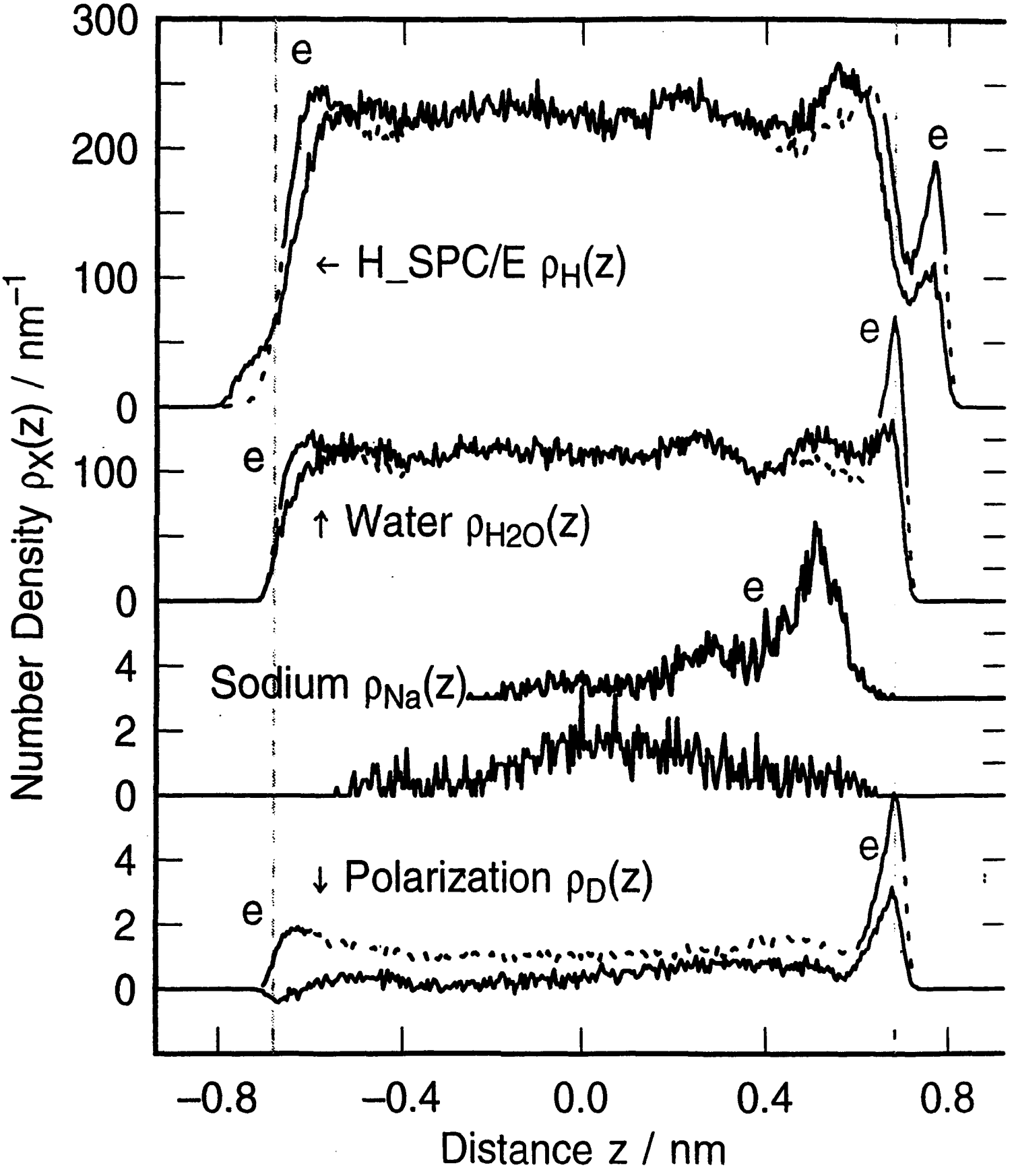
300
200
100
0
100
0
4
2
0
4
2
0
e
e
e
e
e
e
e
← H_SPC/E $\rho_H(z)$
↑ Water $\rho_{H2O}(z)$
Sodium $\rho_{Na}(z)$
↓ Polarization $\rho_D(z)$
Number Density $\rho_X(z)$ / nm^{-1}
–0.8
–0.4
0.0
0.4
0.8
Distance z / nm

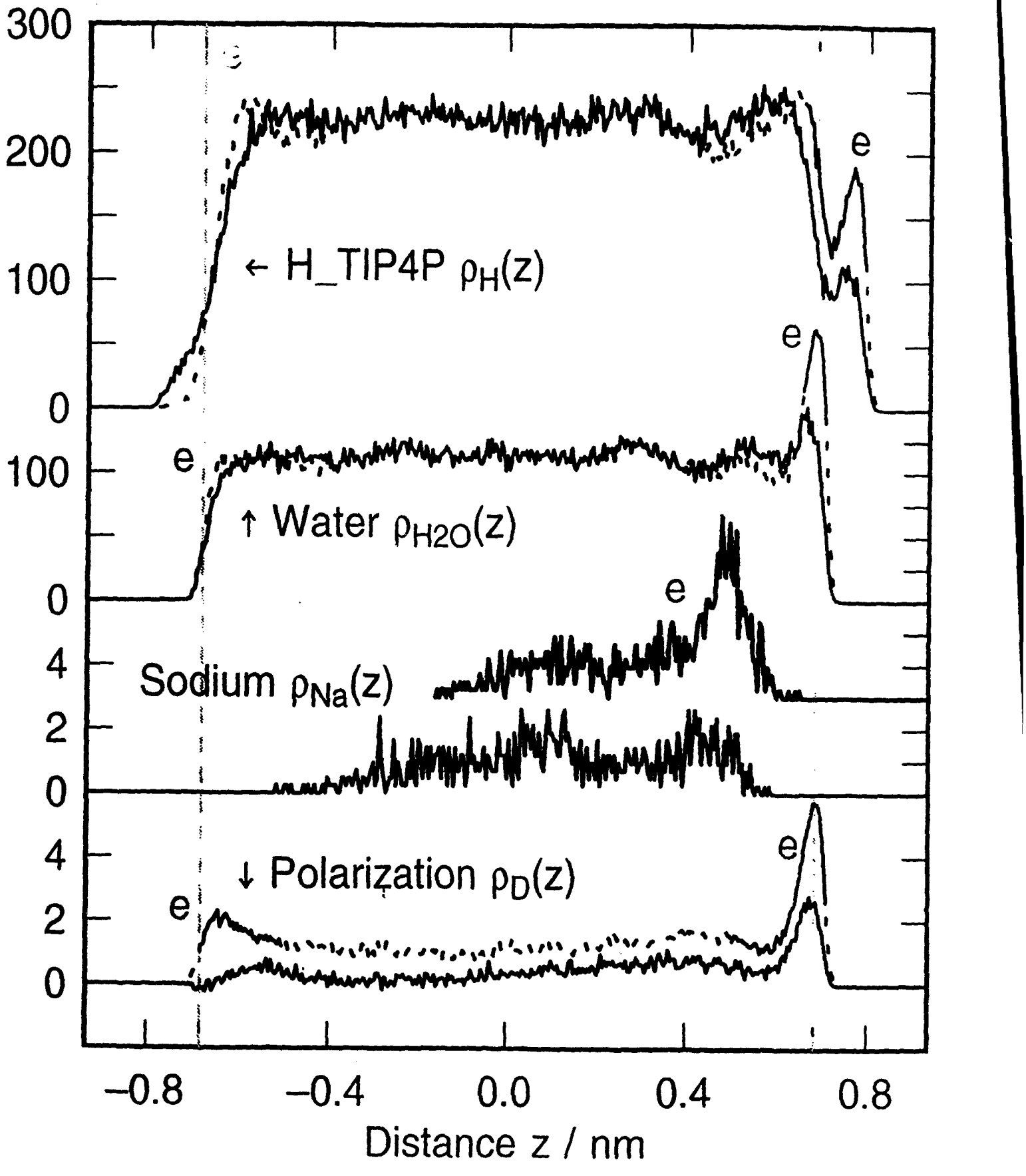
300
200
100
0
100
0
4
2
0
4
2
0
e
e
e
e
e
e
← H_TIP4P $\rho_H(z)$
↑ Water $\rho_{H2O}(z)$
Sodium $\rho_{Na}(z)$
↓ Polarization $\rho_D(z)$
–0.8
–0.4
0.0
0.4
0.8
Distance z / nm

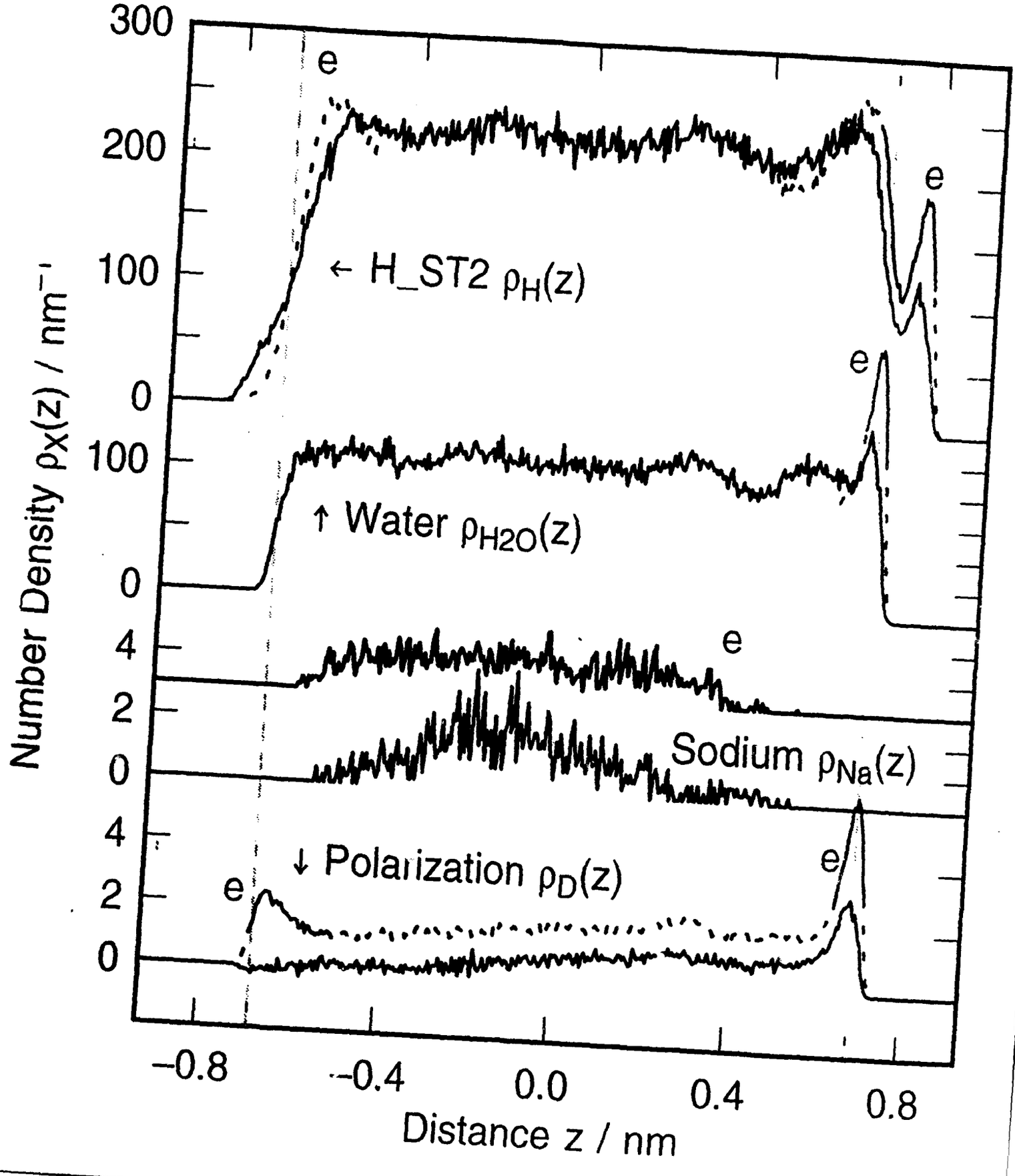
300
200
100
0
100
0
4
2
0
4
2
0
e
e
e
e
e
e
← H_ST2 $\rho_H(z)$
↑ Water $\rho_{H2O}(z)$
Sodium $\rho_{Na}(z)$
↓ Polarization $\rho_D(z)$
Number Density $\rho_X(z)$ / nm^{-1}
−0.8
−0.4
0.0
0.4
0.8
Distance z / nm

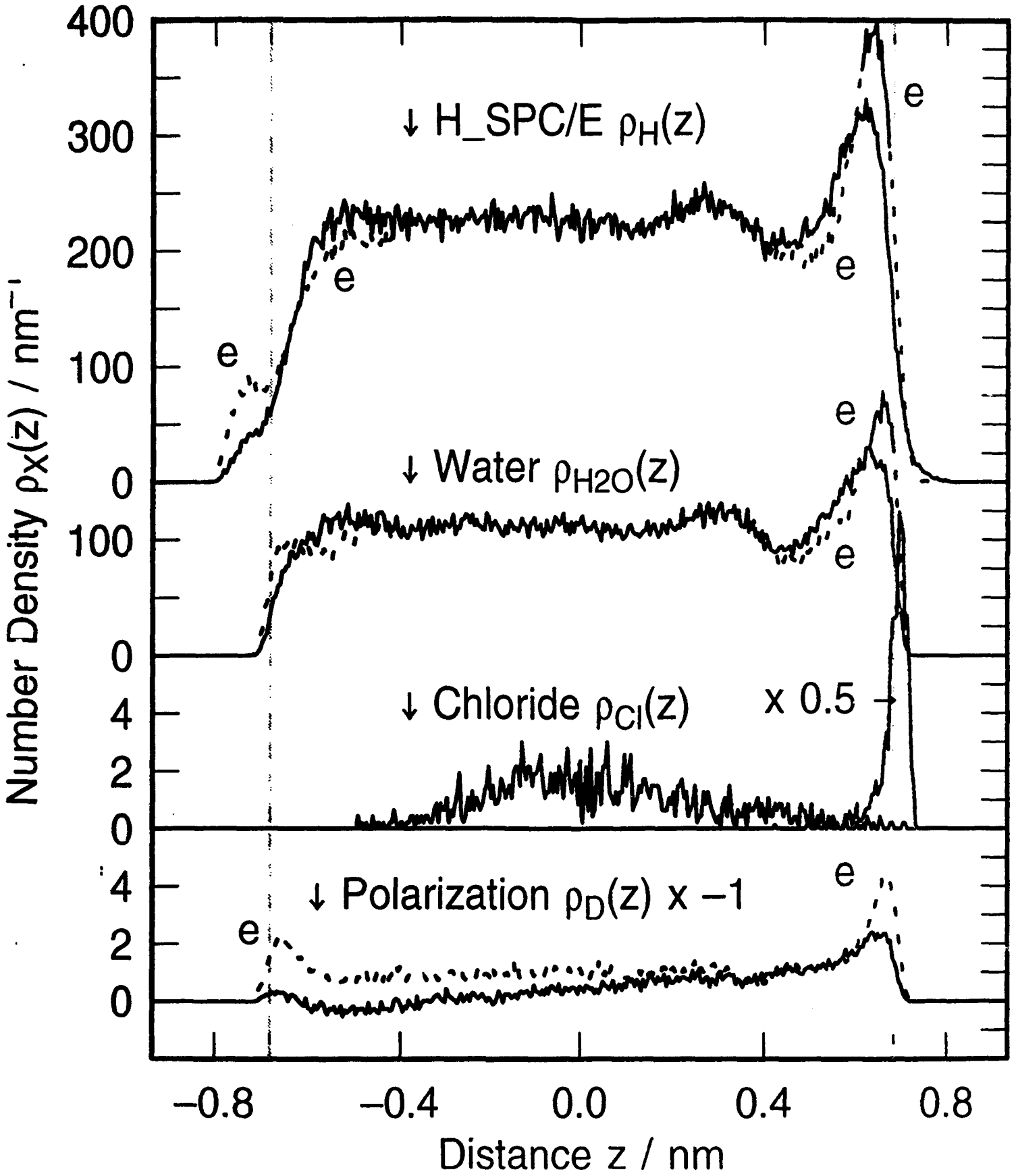
400
300
200
100
0
100
0
4
2
0
4
2
0
↓ H_SPC/E $\rho_H(z)$
↓ Water $\rho_{H2O}(z)$
↓ Chloride $\rho_{Cl}(z)$
x 0.5
↓ Polarization $\rho_D(z)$ x −1
e
Number Density $\rho_X(z)$ / nm^{-1}
−0.8
−0.4
0.0
0.4
0.8
Distance z / nm

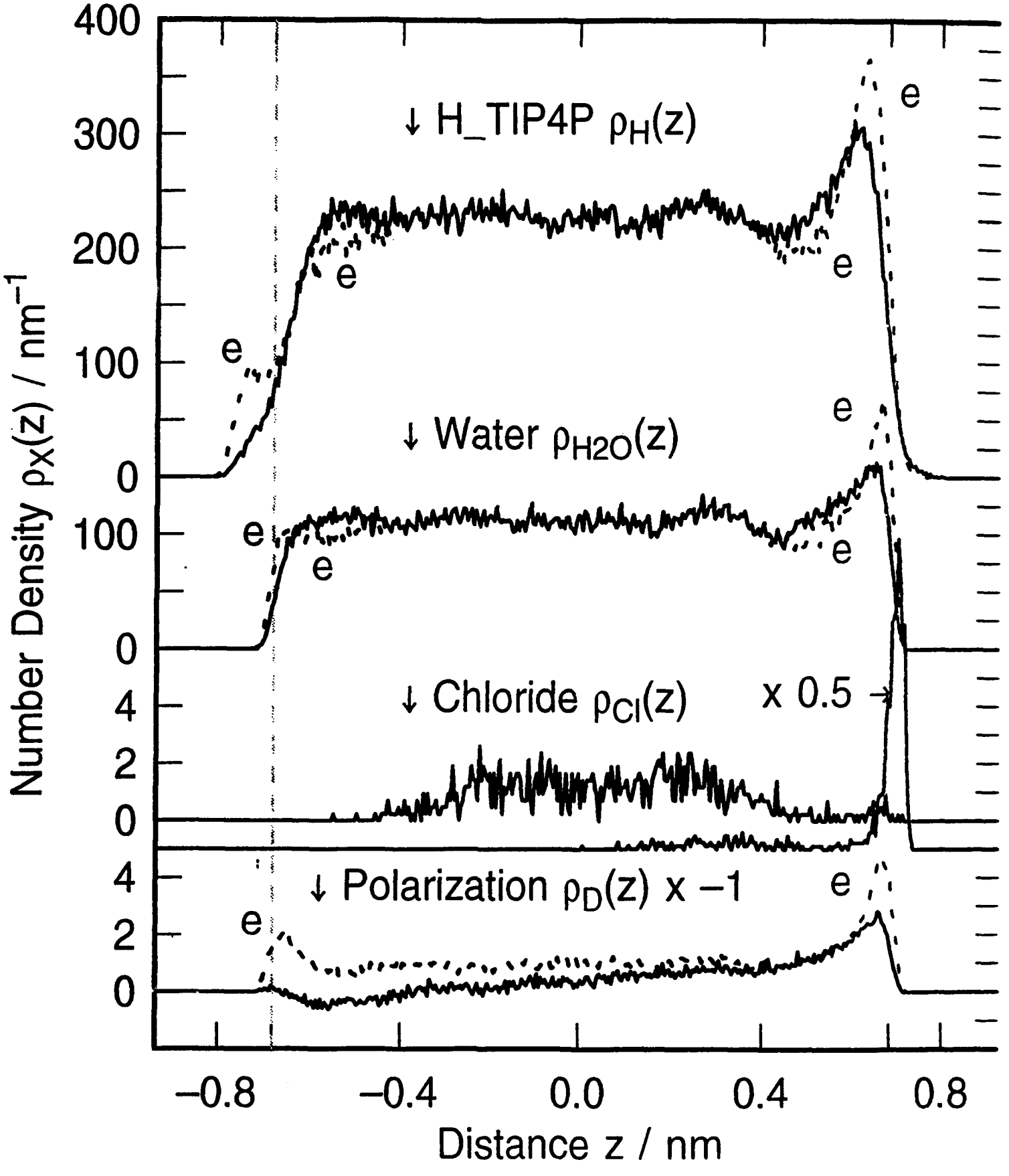
400
300
200
100
0
100
0
4
2
0
4
2
0
↓ H_TIP4P $\rho_H(z)$
↓ Water $\rho_{H2O}(z)$
↓ Chloride $\rho_{Cl}(z)$
x 0.5
↓ Polarization $\rho_D(z)$ x −1
e
Number Density $\rho_X(z)$ / nm^{-1}
−0.8
−0.4
0.0
0.4
0.8
Distance z / nm

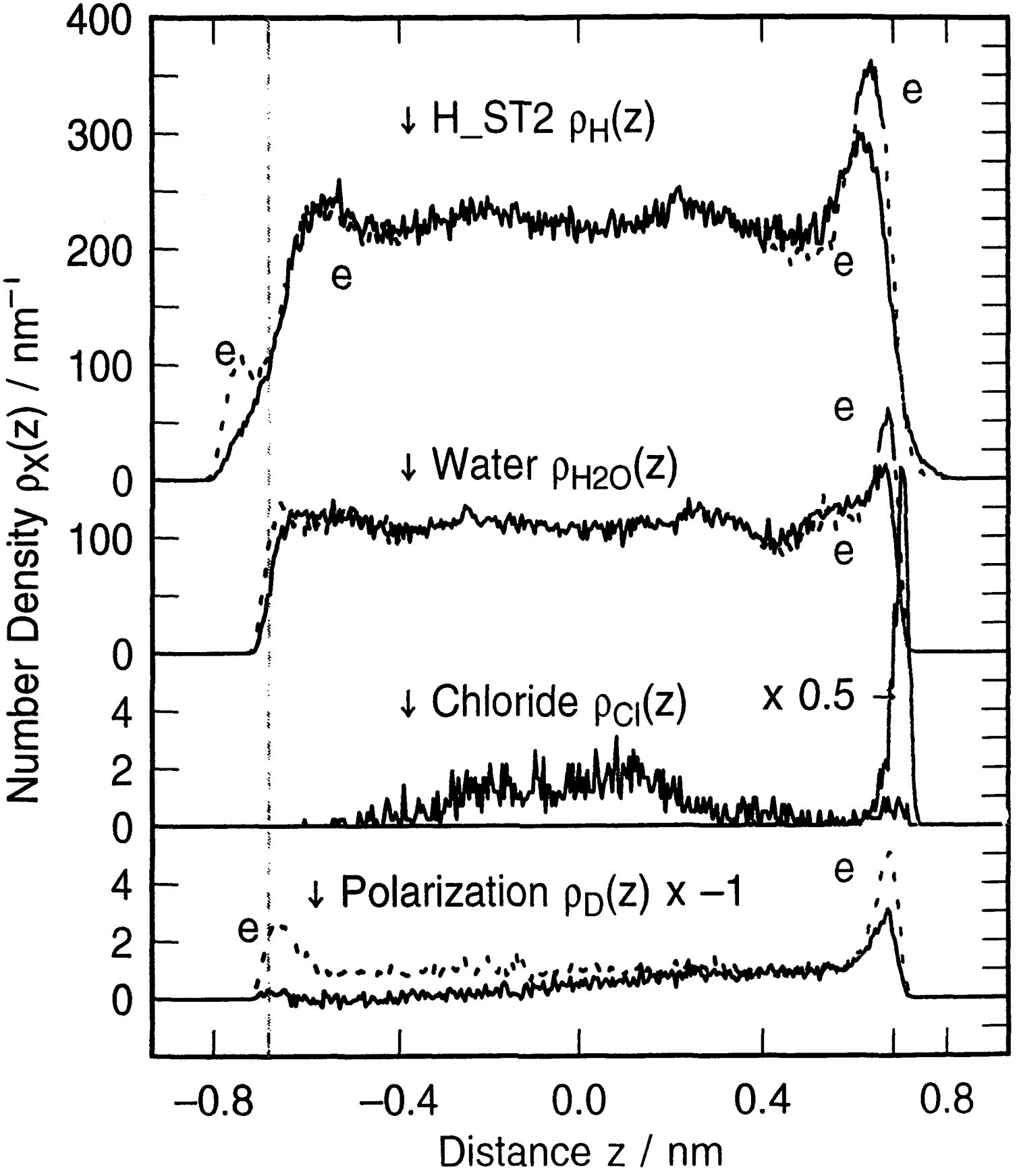
400
300
200
100
0
100
0
4
2
0
4
2
0
↓ H_ST2 $\rho_H(z)$
↓ Water $\rho_{H2O}(z)$
↓ Chloride $\rho_{Cl}(z)$
x 0.5
↓ Polarization $\rho_D(z)$ x −1
e
Number Density $\rho_X(z)$ / nm^{-1}
−0.8
−0.4
0.0
0.4
0.8
Distance z / nm

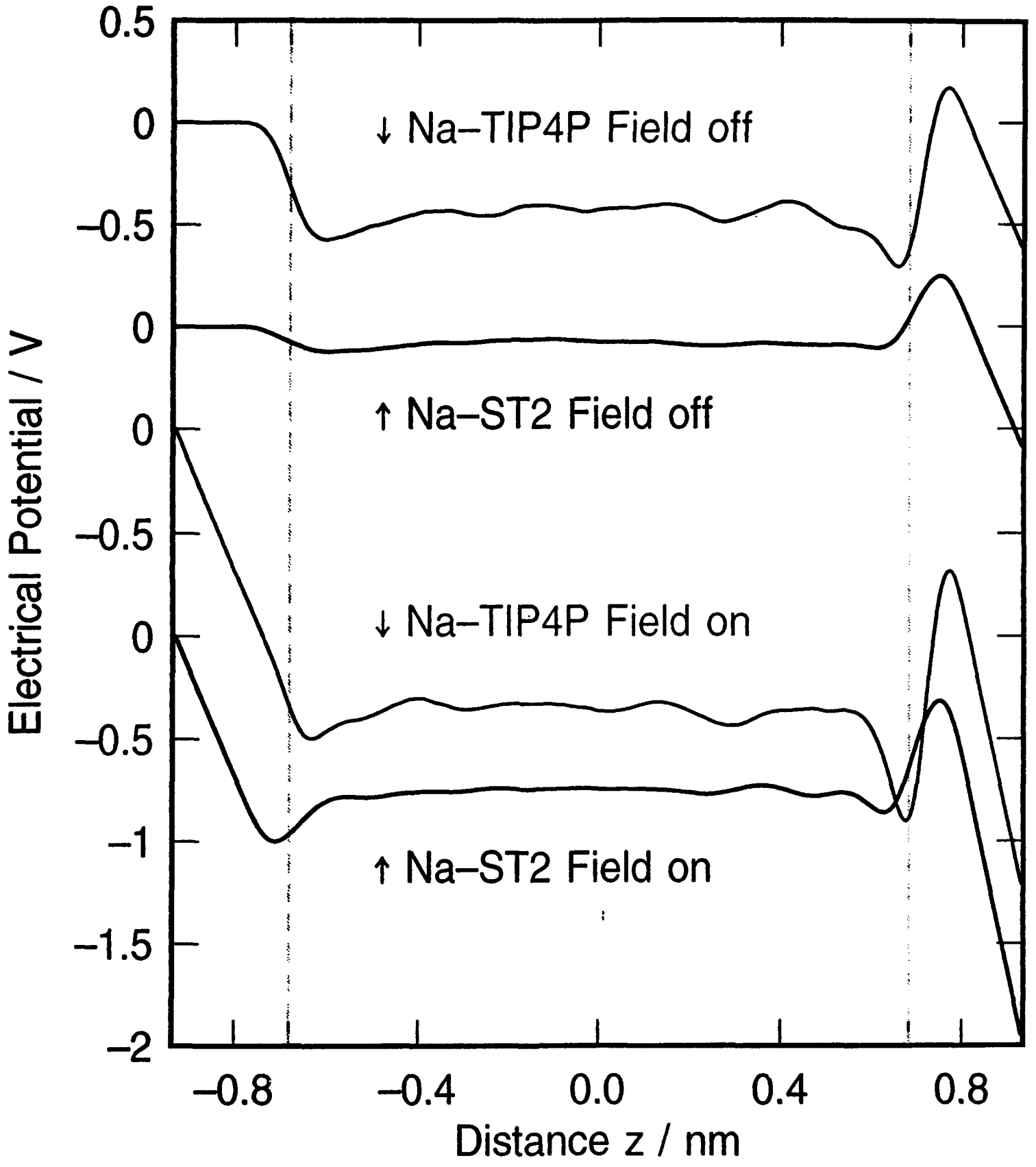
0.5
0
−0.5
0
0
−0.5
0
−0.5
−1
−1.5
−2
↓ Na–TIP4P Field off
↑ Na–ST2 Field off
↓ Na–TIP4P Field on
↑ Na–ST2 Field on
Electrical Potential / V
−0.8
−0.4
0.0
0.4
0.8
Distance z / nm